Reactivated lithospheric-scale discontinuities localize dynamic uplift of the Moroccan Atlas Mountains

Meghan S. Miller and Thorsten W. Becker
Department of Earth Sciences, University of Southern California, 3651 Trousdale Parkway, MC704, Los Angeles, California 90089, USA

ABSTRACT

The Atlas Mountains of Morocco, an example of an intracontinental mountain belt, display only modest tectonic shortening, yet have unusually high topography. We present new evidence from receiver functions and shear-wave splitting for localized, nearly vertical offset deformation of both crust-mantle and lithosphere-asthenosphere interfaces at the flanks of the High Atlas. These offsets coincide with the locations of Jurassic-aged normal fault reactivation that led to tectonic inversion of the region during the Cenozoic. This suggests that a lithospheric-scale discontinuity is involved in orogeny. Another significant step in lithospheric thickness is inferred within the Middle Atlas. Its location corresponds to the source of regional Quaternary alkali volcanism, where the influx of melt induced by the shallow asthenosphere appears to be restricted to the lithospheric-scale fault on the northern side of the range. Inferred stretching axes from shear-wave splitting are aligned with the highest topography, suggesting along-strike asthenospheric shearing in mantle flow guided by lithospheric topography. Isostatic modeling based on these improved crustal thickness and offset estimates indicates that lithospheric thinning alone does not explain the anomalous Atlas topography. Instead, an upwelling component induced by a hot mantle anomaly is also required to support the Atlas, suggesting that the timing of uplift is contemporaneous with the recent volcanism in the Middle Atlas. These observations provide a refined understanding of intracontinental orogeny and localized volcanism.

INTRODUCTION

Major orogens such as the Himalayas and Andes result from significant crustal thickening close to plate boundaries and are associated with substantial relative plate convergence. However, lateral strength variations of the continental lithosphere, such as those due to failed rifts or lithospheric delamination, are likely to modify lithospheric strain localization. Such zones of localized weakness may guide the formation of high topography away from plate boundaries, where orogeny may be driven by upper mantle small-scale convection, such as lithospheric removal and asthenospheric upwellings (cf. Butler et al., 1997; Levander and Miller, 2012; Karlstrom et al., 2012). The Atlas Mountains of Morocco (Fig. 1) consist of the east-northeast–trending High Atlas and the northeast-trending Middle Atlas, which is an intracontinental compressional belt formed by reactivation of synrift Jurassic-age normal faults during the Cenozoic when Africa collided with Eurasia (Brede et al., 1992; Gomez et al., 2000; Pique et al., 2002; Teixell et al., 2003). Due to their lack of nappes, flysch sediments, ophiolites, and granitoid intrusions, and the distance from the collision zone, the Atlas Mountains have traditionally been differentiated from the collisional orogens such as the Alpine belts. The elevation of the mountain range peaks at more than 4100 m, yet the orogenic shortening is small (15%–25%) and the Moho thickness across the Atlas is modest (average ~35 km), and therefore inconsistent with Airy isostatic support of the present-day elevation and recent uplift history (Sandvol et al., 1998; Beauchamp et al., 1999; Gomez et al., 2000; Sebrier et al., 2006).

The southern side of the High Atlas is bounded by the South Atlas fault zone, which is a major tectonic feature that extends from western Morocco, where the High Atlas belt is juxtaposed to the Anti-Atlas Mountains and West African craton to the south, to Tunisia. The shortening across the Atlas is overall asymmetric, the South Atlas fault zone generally accommodating more Cenozoic shortening and active tectonic deformation than the northern side (Sebrier et al., 2006). There, the strike of the Middle Atlas diverges at an angle to the central High Atlas (Figs. 1 and 2), and can be subdivided into three regions: from north to south, these are the Tabular Middle Atlas, which consist of generally

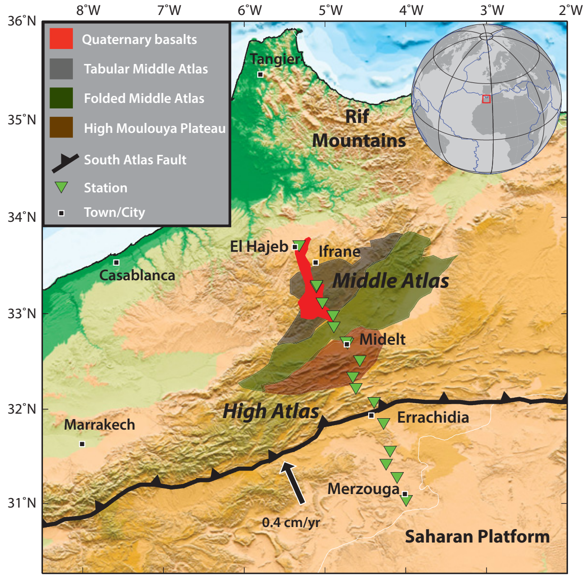

Figure 1. Generalized tectonic map with seismic stations (triangles), major cities, and tectonic regions from Gomez et al. (1998). South Atlas fault is indicated with a black line; Quaternary basalt outcrops (Fullea et al., 2010) are shown in red. Arrow indicates Cenozoic convergence (Rosenbaum et al., 2002); global map inset shows study region outlined by a red box and the major plate boundaries.

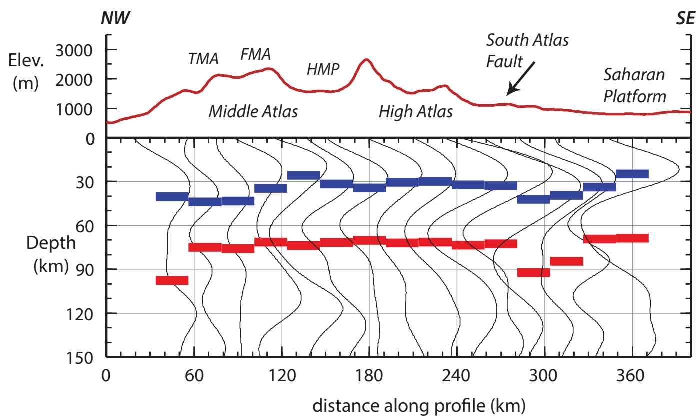

Figure 2. S-receiver function profile across Atlas Mountains from northwest to southeast; top panel indicates tectonic features and elevation. HMP—High Moulouya platform; FMA—folded Middle Atlas; TMA—Tabular Middle Atlas (cf. Fig. 1). Receiver function stacks at 40 km spacing are shown for all stations within 20 km of profile and plotted evenly spaced for clarity. Blue and red dashes indicate Moho and lithosphere-asthenosphere boundary, respectively.

Data Repository item 2014009 | doi:10.1130/G34959.1

flat lying Mesozoic sedimentary rocks, the High Moulouya platform, which consist of similar subhorizontal strata, and the folded Middle Atlas, where most of the deformation of the mountain belt is exposed (following Gomez et al., 1998). The Tabular Middle Atlas are the loci of Quaternary alkali volcanism (Anguita and Hernan, 2000; Duggen et al., 2009) suggested to be contemporaneous with the uplift of the Atlas (Beauchamp et al., 1999). However, this tectonic domain has undergone less deformation than the higher topography regions of the High Atlas and Middle Atlas (Gomez et al., 1998).

In order to understand the tectonic evolution and lithospheric structure of the Atlas Mountains, a linear array of seismic stations was deployed from 2009 through 2013 (Fig. 1). This array of broadband seismometers across the central High Atlas, between Merzouga and El Hajeb (Fig. 1), extended perpendicular to the axis of the mountain belt and parallel to the direction of convergence during the Cenozoic (Rosenbaum et al., 2002). This geometry is ideal for imaging of the bounding structure of the mountain range at the required lithospheric-scale depths.

SEISMOLOGICAL CONSTRAINTS

Recent P-wave tomography (Bezada et al., 2013) based on the linear array of stations across the Atlas and additional seismometers from an areal array deployment in Spain and central Morocco (National Science Foundation PICASSO [Program to Investigate Convective Alboran Sea System Overturn] and IberArray [TopoIberia seismic networks]) suggests that there is a localized low-velocity anomaly (~–3%) at ~75 km depth beneath the Middle Atlas. This feature is positioned within a more widespread low-velocity anomaly that follows the trend of the entire Atlas and extends to ~160 km depth. Rayleigh wave tomography (Palomeras et al., 2013), based on the same stations used by Bezada et al. (2013), images the lithospheric structure in more detail and also shows a prominent low shear-wave velocity anomaly (~4.1 km/s) between ~45 and 100 km located beneath the central Atlas.

Receiver Function Imaging

The receiver function method can isolate converted waves produced by seismic velocity discontinuities (Langston, 1977; Vinnik, 1977). S-receiver functions have emerged as an effective tool for mapping the lithospheric structure and thickness (cf. Li et al., 2007; Rychert et al., 2007; Levander and Miller, 2012). Because the converted P phases appear as precursors to the main S phase, they do not undergo multiple contamination like P receiver functions. To image the lithospheric structure beneath the Atlas we use 67 teleseismic events with magnitude (M_w) >6 at a distance of 55°–85° from the array. Following the methodology described in Levander and Miller (2012), three component waveforms were visually inspected in the appropriate time window around direct S for clear S-wave arrivals, and then the time series were transformed from Z, N, and E to P, SV, and SH components. S-receiver functions were produced by deconvolving the SV component from the P component in the frequency domain (following Langston, 1977). Receiver functions were depth converted using a one-dimensional model, *ak135* (Kennett et al., 1995), which approximates the Moroccan continental lithosphere (cf. Bezada et al., 2013; Palomeras et al., 2013). The S-receiver functions were rated by quality and stacked at each station by back-azimuth quadrants. The stacks with above-average quality were used to hand-pick the Moho and the lithosphere asthenosphere boundary. All S-receiver function–based interface depth estimates are available in Table DR1 in the GSA Data Repository[1].

Our S-receiver function imaging shows that the lithosphere is thin (~65 km) beneath the Middle and High Atlas, but thickens to ~100 km over a very short distance, at both the southern and northern margins of the Atlas Mountains (Figs. 2 and 3C). The crustal thickness interpretations from the S-receiver functions show an average of ~35 km, consistent with both P-receiver function and seismic refraction estimates (Sandvol et al., 1998; S. Thurner, 2013, personal commun.; Carbonell et al., 2013), although individual stations along the profile show more variability. The thinnest portion of the crust (~25 km) is located beneath the Middle Atlas, specifically the High Moulouya platform (Figs. 2 and 3C), opposite to what would be expected from the (Airy) isostatic adjustment of a constant density crust. The estimated depth to the asthenosphere from the deeper impedance contrast, the inferred lithosphere-asthenosphere boundary, broadly matches inferences from regional tomography models (Sebrier et al., 2006; Bezada et al., 2013; Palomeras et al., 2013), geophysical

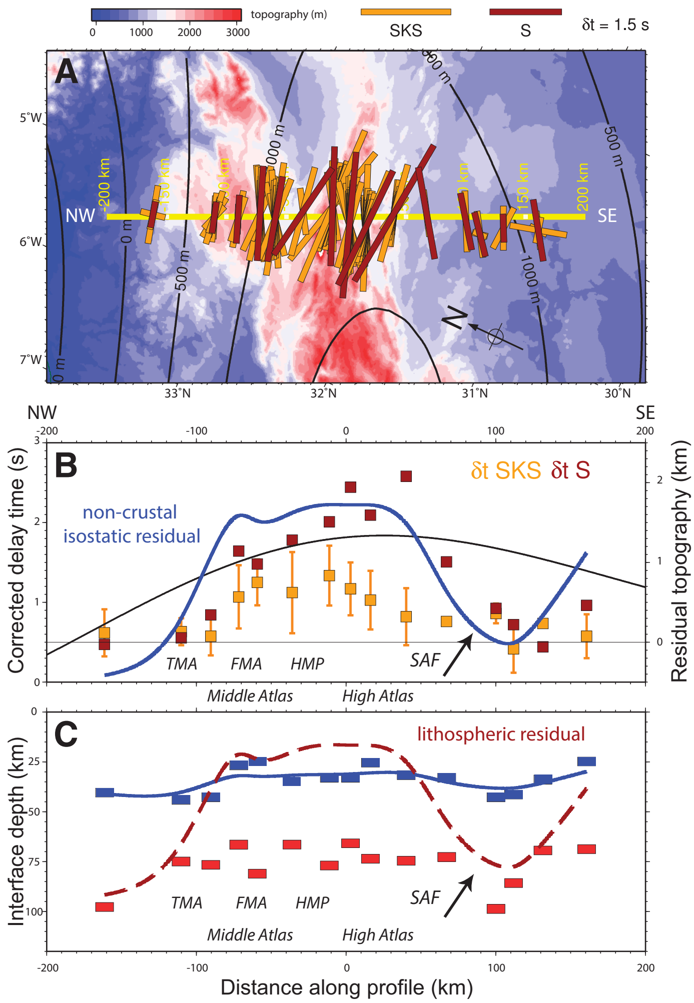

Figure 3. A: Map of stations (oblique Mercator projection) with SKS (orange) and S (dark red) splitting measurements (Miller et al., 2013). Fast polarization and delay times (δ*t*) are denoted by stick orientation and length. Background shading is actual topography, black contours are gravity-inferred residual topography (as in Craig et al., 2011), and yellow line shows profile used in B and C. B: Above 410 km path length corrected splitting delay times for S and SKS; black and blue lines show free-air gravity and crustal (Airy) isostatic residual topography, respectively. Scale is the same as in C. TMA—Tabular Middle Atlas; FMA—folded Middle Atlas; HMP—High Moulouya platform; SAF—South Atlas fault. C: Picks for the Moho (blue) and lithosphere-asthenosphere boundary (red) from S-receiver functions (see Fig. 2); blue line shows fit to Moho used for crustal residual in B. Dark red dashed line shows inferred lithospheric thickness from isostasy assuming zero mantle-induced dynamic contribution to residual topography in B.

[1]GSA Data Repository item 2014009, seismic station location, quality of SRF stack, and depths to discontinuities, is available online at www.geosociety.org/pubs/ft2014.htm, or on request from editing@geosociety.org or Documents Secretary, GSA, P.O. Box 9140, Boulder, CO 80301, USA.

modeling of gravity and heat-flow data (Teixell et al., 2005; Missenard et al., 2006; Fullea et al., 2010), as well as results from some deep electrical resistivity studies (Anahnah et al., 2011), although the latter are debated (Jones et al., 2012).

On the southern side of the Atlas, we find strikingly consistent steps in both crustal and lithospheric thickness that occur across the South Atlas fault (Figs. 2 and 3C). Both the crust and lithosphere are markedly thinner beneath the Atlas than beneath the Saharan platform; the offset in the crust is ~9 km and the offset in the lithosphere is ~26 km crossing the bounding thrust fault north of Errachidia (Fig. 1). At the northern margin of the Atlas, the lithosphere has a significant step of ~23 km between El Hajeb and the boundary of the Tabular Middle Atlas (Figs. 2 and 3C). However, cross sections based on structural geology and seismic reflection data that span the boundaries of the Atlas demonstrate only moderately to shallowly dipping thrust faults, particularly along the flanks of the High Atlas (Beauchamp et al., 1999; Frizon de Lamotte et al., 2009). Our S-receiver function analysis also shows an abrupt change in lithospheric (~10 km) and crustal (~16 km) thicknesses at the boundary between the folded Middle Atlas and the High Moulouya platform, previously undetected by other geophysical imaging methods.

Shear-Wave Splitting

Shear-wave splitting analysis is based on the fact that shear waves are split into a fast and a slow pulse upon propagation through azimuthally anisotropic portions of the lithosphere or upper mantle (e.g., Vinnik et al., 1984; Silver and Chan, 1991). The two orthogonal shear pulses propagate at different velocities and are polarized into the corresponding fast (φ) and slow polarization orientations of the rocks through which they are traveling. The delay time (δt) between the arrival of the two pulses as recorded at the seismic station is indicative of the path-integrated anisotropy strength, and the combination of delay times and fast polarization orientations can be used to infer seismic anisotropy in the upper mantle. We (Miller et al., 2013) conducted shear-wave splitting analyses for direct S (from the deep focus 11 April 2010 event beneath Granada, Spain) and 235 teleseismic SKS events recorded across the Atlas (Fig. 1) using the SplitLab toolkit (Wüstefeld et al., 2008). Both SKS and S measurements display consistent delay time patterns where the largest amplitudes correlate with the largest anomalous topography along the profile, but then systematically decrease in magnitude at the flanks of the mountain range (Figs. 3A and 3B). The two most abrupt decreases in delay times correspond to the position of the South Atlas fault zone, which marks the southern margin of the Atlas, and the boundary between the folded Middle Atlas and the High Moulouya platform (Figs. 3A and 3B), which is where we also observe the large offsets in the crust and lithosphere from the S-receiver function analysis.

DYNAMIC TOPOGRAPHY

We use our improved crustal and lithospheric structure estimates along with our seismic anisotropy observations to provide some further geodynamic inferences on the Atlas orogeny. Because we are interested in long-term deformation, we minimize flexural topography effects by means of long-wavelength filtering (Gaussian with 6σ width of 150 km), and Figure 3C shows such a fit to the Moho estimates from the S-receiver functions (blue line). Using typical densities for crust (2800 kg/m^3) and mantle lithosphere (3270 kg/m^3), we can adjust the asthenospheric density to maximize the fit between Airy-balanced crustal predictions and smoothed observed topography. With a reference ridge bathymetry of −2.6 km (sea level) and mean total lithospheric thickness of 78 km, a best-fit asthenospheric density is 3177 kg/m^3. (For details of the computation and trade-offs of such models see, e.g., the discussion in Lachenbruch and Morgan, 1990.) This seismology-guided estimate of the residual topography that is not isostatically balanced by crustal thickness variations is shown in blue in Figure 3B, alongside an independent inference of dynamic topography, based on filtered free-air gravity (following Craig et al., 2011), shown in black.

We ask if lithospheric thickness variations are sufficient to explain the residual Atlas topography. Such a model is plotted as the dashed red curve of Figure 3C, assuming that all residual topography is caused by static lithospheric mantle thickness reduction at constant density. While the shape of the inferred lithosphere-asthenosphere boundary matches the inferences from the receiver functions, the amplitude variations of this model are implausible, and in places inconsistent with (i.e., shallower than) the crustal thickness. The effects of lateral density variations within the lithosphere, due to higher lithospheric temperatures or partial melting that are inferred from volcanism (Anguita and Hernan, 2000; Duggen et al., 2009) and resistivity modeling (Anahnah et al., 2011) may explain part of the residual. However, the equivalent lithospheric density anomalies required to explain all topography in terms of a static compensation are ~2%–3%, likely too large to be associated with such effects (Afonso and Schutt, 2012). It may be possible to adjust the density structure of the lithosphere and other parameters to partially reduce the extent of unrealistic lithospheric thickness (cf. Fullea et al., 2010), but it seems unlikely that the entire topography residual is static in origin. This implies a convective cause, i.e., support of topography by mantle tractions due to an active mantle upwelling.

DISCUSSION

Our study confirms that the Atlas cannot be in Airy isostatic balance. We constrain maximum positive topography residuals, and find that those coincide with a regional maximum of seismic anisotropy and offsets in the crust and lithosphere thickness along the margins of the High Atlas and the central Middle Atlas. The inferred stretching axes from anisotropy are aligned with surface topography, consistent with northeast-southwest–oriented shearing in mantle flow in the asthenosphere, perhaps guided by lithospheric topography. Such a type of flow has been associated with lithospheric delamination, or erosion of a lithospheric root, perhaps in conjunction with a northward progression of hot Canary plume material (Duggen et al., 2009). An associated mantle thermal anomaly may be the source of localized volcanism in the Middle Atlas (Beauchamp et al., 1999).

We take our results from topography modeling, lithospheric structure from receiver functions, and shear wave splitting to imply that support of the anomalous topography of the Atlas at present has to mainly reside in upper mantle convection, where upward flow associated with a relatively hot asthenosphere is supporting the mountain belt. This flow is likely guided by preexisting lithospheric heterogeneities and abrupt thickness variations at the edges of the Atlas. A hot anomaly underneath the Atlas will not only provide a buoyancy source, but also locally reduce the viscosity of the mantle, and so lead to increased strain rates at constant pressure difference, perhaps channeling the larger scale upwelling that is feeding volcanism in the Canary hotspot (Duggen et al., 2009), thus explaining the increased splitting delay times underneath the Atlas. This convective current appears to be guided by lithospheric structure on multiple spatial scales, including the strong cratonic keel to the south (Alpert et al., 2013), and may be enhanced by suction from slab segmentation in the Alboran domain (Duggen et al., 2009). Such enhanced convective activity may allow for local erosion and root removal of a previously thickened lithosphere underneath the Atlas, and reactivate the bounding Jurassic-age normal faults in the crust (Brede et al., 1992; Gomez et al., 2000; Pique et al., 2002; Teixell et al., 2003). The present-day step in lithospheric thickness within the Middle Atlas appears to correspond to the source of regional Quaternary alkali volcanism (Anguita and Hernan, 2000; Duggen et al., 2009) that is restricted to the northern side of the mountain belt. This offset is consistent with the position of melt chambers as inferred from inversion of electrical resistivity measurements (Anahnah et al., 2011), suggesting that the timing of uplift of the Atlas is contemporaneous with this recent volcanism. More generally, this case history illustrates how reactivated localization of deformation through the entire lithosphere can contribute to mountain building within a region of vigorous upper mantle convection, which may be relevant to other regions.

ACKNOWLEDGMENTS

We thank the PICASSO (National Science Foundation [NSF] Program to Investigate Convective Alboran Sea System Overturn) group and our collaborators at l'Institut Scientifique á Rabat. This study was supported by NSF Continental Dynamics Program grant EAR-0809023.

REFERENCES CITED

Afonso, J.C., and Schutt, D.L., 2012, The effects of polybaric partial melting on density and seismic velocities of mantle restites: Lithos, v. 134–135, p. 289–303, doi:10.1016/j.lithos.2012.01.009.

Alpert, L.A., Miller, M.S., Becker, T.W., and Allam, A., 2013, Structure beneath the Alboran from geodynamic flow models and seismic anisotropy: Journal of Geophysical Research, v. 118, p. 1–13, doi:10.1002/jgrb.50309.

Anahnah, F., and 17 others, 2011, Deep resistivity cross section of the intraplate Atlas Mountains (NW Africa): New evidence of anomalous mantle and related Quaternary volcanism: Tectonics, v. 30, doi:10.1029/2010TC002859.

Anguita, F., and Hernan, F., 2000, The Canary Islands origin: A unifying model: Journal of Volcanology and Geothermal Research, v. 103, p. 1–26, doi:10.1016/S0377-0273(00)00195-5.

Beauchamp, W., Allmendinger, R.W., Barazangi, M., Demnati, A., El Alji, M., and Dahmani, M., 1999, Inversion tectonics and the evolution of the High Atlas Mountains, Morocco, based on a geological-geophysical transect: Tectonics, v. 18, p. 163–184, doi:10.1029/1998TC900015.

Bezada, M.J., Humphreys, E.D., Toomey, D.R., Harnafi, M., Dávila, J.M., and Gallart, J., 2013, Evidence for slab rollback in westernmost Mediterranean from improved upper mantle imaging: Earth and Planetary Science Letters, v. 368, p. 51–60, doi:10.1016/j.epsl.2013.02.024.

Brede, R., Hauptmann, M., and Herbig, H.-G., 1992, Plate tectonics and intracratonic mountain ranges in Morocco—The Mesozoic–Cenozoic development of the Central High Atlas and the Middle Atlas: Geologische Rundschau, v. 81, p. 127–141, doi:10.1007/BF01764544.

Butler, R.W.H., Holdsworth, R.E., and Lloyd, G.E., 1997, The role of basement reactivation in continental deformation: Geological Society of London Journal, v. 154, p. 69–71, doi:10.1144/gsjgs.154.1.0069.

Carbonell, R., and 10 others, 2013, A 700 km long crustal transect across northern Morocco: Vienna, EGU General Assembly, Volume 15, p. EGU2013–8313.

Craig, T.J., Jackson, J.A., Priestley, K., and McKenzie, D.P., 2011, Earthquake distribution patterns in Africa: Their relationship to variations in lithospheric and geological structure, and their rheological implications: Geophysical Journal International, v. 185, p. 403–434, doi:10.1111/j.1365-246X.2011.04950.x.

Duggen, S., Hoernle, K.A., Hauff, F., Klügl, A., Bouabdellah, M., and Thirlwall, M., 2009, Flow of Canary mantle plume material through a subcontinental lithospheric corridor beneath Africa to the Mediterranean: Geology, v. 37, p. 283–286, doi:10.1130/G25426A.1.

Frizon de Lamotte, D., Leturmy, P., Missenard, Y., Saddiqi, O., Guillocheau, F., and Michard, A., 2009, Mesozoic and Cenozoic vertical movements in the Atlas system (Algeria, Morocco, Tunisia): An overview: Tectonophysics, v. 475, p. 9–28, doi:10.1016/j.tecto.2008.10.024.

Fullea, J., Fernandez, M., Afonso, J.C., Verges, J., and Zeyen, H., 2010, The structure and evolution of the lithosphere-asthenosphere boundary beneath the Atlantic-Mediterranean transition region: Lithos, v. 120, p. 74–95, doi:10.1016/j.lithos.2010.03.003.

Gomez, F., Allmendinger, R.W., Barazangi, M., Er-Raji, A., and Dahmani, M., 1998, Crustal shortening and vertical strain partitioning in the Middle Atlas Mountains of Morocco: Tectonics, v. 17, p. 520–533, doi:10.1029/98TC01439.

Gomez, F., Beauchamp, W., and Barazangi, M., 2000, Role of the Atlas Mountains (northwest Africa) within the African-Eurasian plate-boundary zone: Geology, v. 28, p. 775–778, doi:10.1130/0091-7613(2000)28<775:ROTAMN>2.0.CO;2.

Jones, A., Kiyan, D., Fullea, J., Ledo, J., Queralt, P., Marcuello, A., Siniscalichi, A., and Romano, G., 2012, Deep resistivity cross section of the intraplate Atlas Mountains (NW Africa): New evidence of anomalous mantle and related Quaternary volcanism: Comment: Tectonics, v. 31, doi:10.1029/2011TC003051.

Karlstrom, K.E., and 24 others, 2012, Mantle-driven dynamic uplift of the Rocky Mountains and Colorado Plateau and its surface response: Toward a unified hypothesis: Lithosphere, v. 4, p. 3–22, doi:10.1130/L150.1.

Kennett, B.L.N., Engdahl, E.R., and Buland, R., 1995, Constraints on seismic velocities in the Earth from travel times: Geophysical Journal International, v. 122, p. 108–124, doi:10.1111/j.1365-246X.1995.tb03540.x.

Lachenbruch, A.H., and Morgan, P., 1990, Continental extension, magmatism and elevation: Formal relation and rules of thumb: Tectonophysics, v. 174, p. 39–62, doi:10.1016/0040-1951(90)90383-J.

Langston, C.A., 1977, Corvallis, Oregon, crustal and upper mantle receiver structure from teleseismic P and S waves: Seismological Society of America Bulletin, v. 67, p. 713–724.

Levander, A., and Miller, M.S., 2012, Evolutionary aspects of the lithosphere discontinuity structure in the Western U.S: Geochemistry Geophysics Geosystems, v. 13, doi:10.1029/2012GC004056.

Li, X., Yuan, X., and Kind, R., 2007, The lithosphere-asthenosphere boundary beneath the western United States: Geophysical Journal International, v. 170, p. 700–710, doi:10.1111/j.1365-246X.2007.03428.x.

Miller, M.S., Allam, A., Becker, T.W., Di Leo, J.F., and Wookey, J., 2013, Constraints on the tectonic evolution of the westernmost Mediterranean and northwestern Africa from shear wave splitting analysis: Earth and Planetary Science Letters, v. 375, p. 234–243, doi:10.1016/j.epsl.2013.05.036.

Missenard, Y., Zeyen, H., Frizon de Lamotte, D., Leturmy, P., Petit, C., Sebrier, M., and Saddiqi, O., 2006, Crustal versus asthenospheric origin of relief of the Atlas Mountains of Morocco: Journal of Geophysical Research, v. 111, no. B3, doi:10.1029/2005JB003708.

Palomeras, I., Thurner, S., Levander, A., Liu, K., Villaseñor, A., and Carbonell, R., 2013, Finite-frequency Rayleigh wave tomography of the Western Mediterranean: Geochemistry Geophysics Geosystems.

Pique, A., Tricart, P., Guiraud, R., Laville, E., Bouaziz, S., Amrhar, M., and AitOuali, R., 2002, The Mesozoic–Cenozoic Atlas belt (North Africa): An overview: Geodinamica Acta, v. 15, p. 185–208, doi:10.1016/S0985-3111(02)01088-4.

Rosenbaum, G., Lister, G.S., and Duboz, C., 2002, Relative motions of Africa, Iberia and Europe during Alpine orogeny: Tectonophysics, v. 359, p. 117–129, doi:10.1016/S0040-1951(02)00442-0.

Rychert, C.A., Rondenay, S., and Fischer, K.M., 2007, P-to-S and S-to-P imaging of a sharp lithosphere-asthenosphere boundary beneath eastern North America: Journal of Geophysical Research, v. 112, doi:10.1029/2006JB004619.

Sandvol, E., Seber, D., Calvert, A., and Barazangi, M., 1998, Grid search modelling of receiver functions: Implications for crustal structure in the Middle East and North Africa: Journal of Geophysical Research, v. 103, p. 26899–26917, doi:10.1029/98JB02238.

Sebrier, M., Siame, L., Zouine, E.M., Winter, T., Missenard, Y., and Leturmy, P., 2006, Active tectonics in the Moroccan High Atlas: Comptes Rendus Geoscience, v. 338, p. 65–79, doi:10.1016/j.crte.2005.12.001.

Silver, P.G., and Chan, W.W., 1991, Shear wave splitting and subcontinental mantle deformation: Journal of Geophysical Research, v. 96, p. 16429–16454, doi:10.1029/91JB00899.

Teixell, A., Arboleya, M.-L., Julivert, M., and Charroud, M., 2003, Tectonic shortening and topography in the central High Atlas (Morocco): Tectonics, v. 22, no. 5, doi:10.1029/2002TC001460.

Teixell, A., Ayarza, P., Zeyen, H., Fernandez, M., and Arboleya, M.-L., 2005, Effects of mantle upwelling in a compressional setting: the Atlas Mountains of Morocco: Terra Nova, v. 17, p. 456–461, doi:10.1111/j.1365-3121.2005.00633.x.

Vinnik, L.P., 1977, Detection of waves converted from P to SV in the mantle: Physics of the Earth and Planetary Interiors, v. 15, p. 39–45, doi:10.1016/0031-9201(77)90008-5.

Vinnik, L.P., Kosarev, G., and Makeyeva, L.I., 1984, Anisotropy of the lithosphere from the observations of *SKS* and *SKKS* phases: USSR Academy of Sciences Proceedings, v. 278, p. 1335–1339.

Wüstefeld, A., Bokelmann, G., Zaroli, C., and Barruol, G., 2008, SplitLab: A shear-wave splitting environment in Matlab: Computers & Geosciences, v. 34, p. 515–528, doi:10.1016/j.cageo.2007.08.002.

Manuscript received 18 July 2013
Revised manuscript received 11 September 2013
Manuscript accepted 13 September 2013

Printed in USA